

Article

Can persistent homology features capture more intrinsic structural information of tumors from CT and PET images of head-and-neck cancer patients?

Quoc Cuong Le¹, Hidetaka Arimura^{2,*}, Kenta Ninomiya³, Takumi Kodama³ and Tetsuhiro Moriyama²

¹ Ho Chi Minh City Oncology Hospital, Ho Chi Minh City, Vietnam

² Department of Health Sciences, Faculty of Medical Sciences, Kyushu University, Japan

³ Department of Health Sciences, Graduate school of Medical Sciences, Kyushu University, Japan

¹ Institute of Mathematics for Industry, Kyushu University, Japan

* Correspondence: arimura.hidetaka.616@m.kyushu-u.ac.jp

Table S1. Histogram-based and texture features used in this study.

	Texture type	Reference(s)	Feature name
14 histogram-based features	-	-	Energy Entropy Kurtosis Maximum Mean Mean absolute difference (MAD) Median Minimum Range Root mean square (RMS) Skewness Standard deviation (STD) Uniformity Variance
45 Texture features	Gray-level co-occurrence matrix (GLCM)	Haralick et al. [1]	Energy Contrast Entropy Homogeneity Correlation
		Haralick et al. [1], Assefa et al. [2]	Sum Average Variance
		Thibault [3]	Dissimilarity
		Aerts et al. [4]	Auto correlation
		Galloway [5]	Short run emphasis (SRE) Long run emphasis (LRE) Gray-level nonuniformity (GLN) Run-length nonuniformity (RLN) Run percentage (RP)
	Gray-level run-length matrix (GLRLM)	Chu et al. [6]	Low gray-level run emphasis (LGRE) High gray-level run emphasis (HGRE)
		Dasarathy and Holder [7]	Short run low gray-level emphasis (SRLGE) Short run high gray-level emphasis (SRHGE)

		Long run low gray-level emphasis (LRLGE) Long run high gray-level emphasis (LRHGE)
	Thibault et al. [8]	Gray-level variance (GLV) Run-length variance (RLV)
Gray-level size zone matrix (GLSZM)	Galloway [5], Thibault et al. [8]	Small zone emphasis (SZE) Large zone emphasis (LZE) Gray-level nonuniformity (GLN) Zone-size nonuniformity (ZSN) Zone percentage (ZP)
	Chu et al. [6], Thibault et al. [8]	Low gray-level zone emphasis (LGZE) High gray-level zone emphasis (HGZE)
	Dasarathy and Holder [7], Thibault et al. [8]	Small zone low gray-level emphasis (SZLGE) Small zone high gray-level emphasis (SZHGE) Large zone low gray-level emphasis (LZLGE) Large zone high gray-level emphasis (LZHGE)
	Thibault et al. [8]	Gray-level variance (GLV) Zone-size variance (ZSV)
Neighborhood gray-tone difference matrix (NGTDM)	Amadasun and King [9]	Coarseness Contrast Busyness Complexity Strength
Neighboring gray-level dependence matrix (NGLDM)	Sun and Wee [10]	Small number emphasis (SNE) Large number emphasis (LNE) Number nonuniformity (NN) Second moment (SM) Entropy

Table S2. Conversion table for clinical variables.

T stage		N stage		TNM stage		HPV	
Character	Numeric	Character	Numeric	Character	Numeric	Character	Numeric
value	value	value	value	value	value	value	value
T0	1	N0	1	I	1	NA	Exclude
T1	2	N1	2	II	2	Negative	1
T2	3	N2	3	III	3	Positive	2
T3	4	N2a	4	IV	4		
T3a	5	N2b	5	IVA	5		
T4	6	N2c	6	IVB	6		
T4a	7	N3	7				
T4b	8	N3a	8				
		N3b	9				

Table S3. Means and standard deviations of intra-class correlation coefficients for conventional, b1, and b1 features.

Conventional features		b0 PH features		b1 PH features	
	Mean		Mean		Mean
	SD		SD		SD
6 bit	0.672	0.229	6 bit_b0_0.0001	0.636	0.269
7 bit	0.656	0.239	6 bit_b0_0.001	0.630	0.284
8 bit	0.651	0.238	6 bit_b0_0.01	0.636	0.275
9 bit	0.636	0.247	6 bit_b0_0.1	0.648	0.269
			6 bit_b0_1	0.750	0.198
			7 bit_b0_0.0001	0.665	0.260
			7 bit_b0_0.001	0.678	0.254
			7 bit_b0_0.01	0.685	0.230
			7 bit_b0_0.1	0.693	0.252
			7 bit_b0_1	0.747	0.215
			8 bit_b0_0.0001	0.690	0.252
			8 bit_b0_0.001	0.682	0.236
			8 bit_b0_0.01	0.664	0.263
			8 bit_b0_0.1	0.729	0.218
			8 bit_b0_1	0.718	0.227
			9 bit_b0_0.0001	0.680	0.258
			9 bit_b0_0.001	0.726	0.224
			9 bit_b0_0.01	0.731	0.222
			9 bit_b0_0.1	0.722	0.228
			9 bit_b0_1	0.706	0.243
			9 bit_b1_1		
				0.686	0.223

Table S4. Best signatures from conventional and PH-based features.

Conventional CT	Conventional PET	Conventional PET/CT
CT_LHH_NGTDM_Busyness	PET_LHH_NGTDM_Strength	CT_LHL_GLSZM,GLV
CT_Hist_Mean		CT_Hist_STD
CT_GLSZM_LZLGE		CT_LHH_GLSZM_LZLGE
CT_LHH_GLRLM_SRLGE		
CT_HHL_GLSZM,GLV		
CT_HLH_Hist_Kurtosis		
PH-CT	PH-PET	PH-PET/CT
CT_b1_HLH_GLCM_Correlation	PET_b0_Hist_Min	PET_b0_HHL_Hist_Mean
	PET_b0_LLL_GLSZM_SZHGE	CT_b1_HLH_Hist_Mean
	PET_b0_HHL_GLSZM_LGZE	PET_b1_LHL_GLCM_AutoCorrelation
	PET_b0_HHL_GLSZM_LZE	

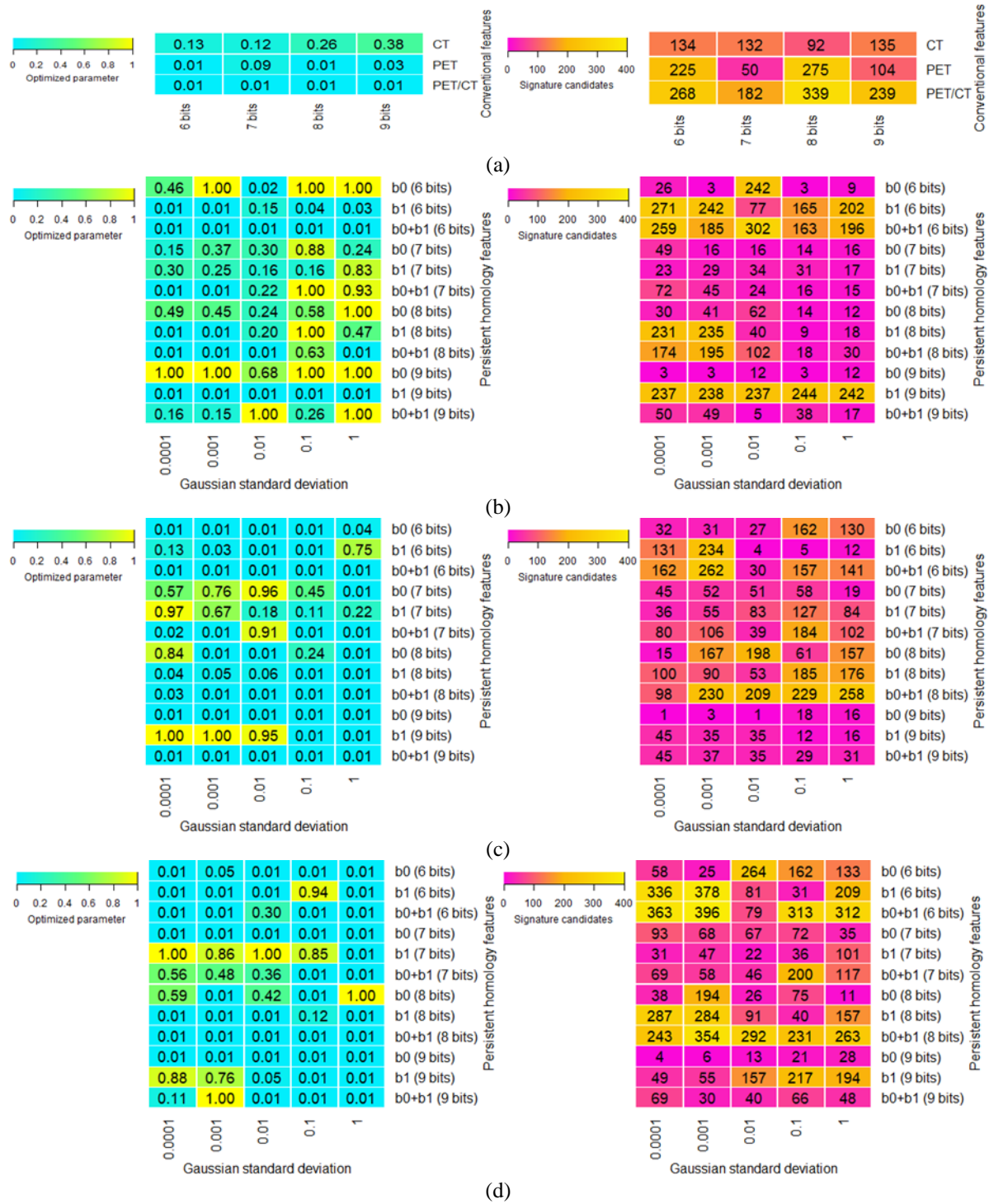


Figure S1. Optimized blending parameter α of the Coxnet model (left) and number of selected signature candidates (right) for 6-, 7-, 8-, and 9- (a) Conventional (CT, PET, and PET/CT), (b) b0 and b1 PH-CT, (c) b0 and b1 PH-PET, and (d) b0 and b1 PH-CT/PET features.

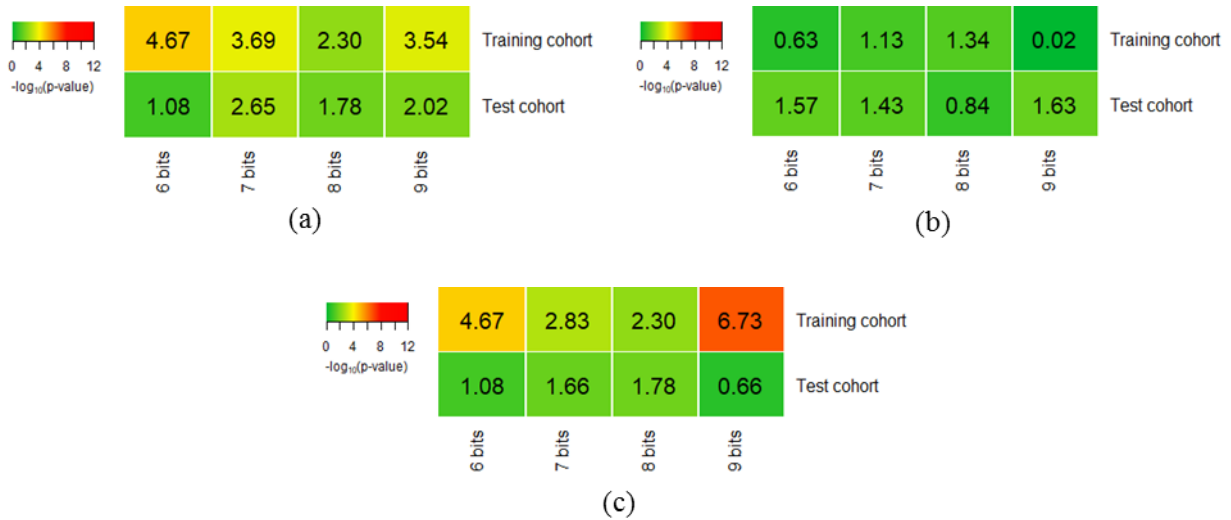


Figure S2. Log-rank p-values in the training and test cohorts of CPHMs built using conventional (a) CT, (b) PET, and (c) PET/CT signatures.



Figure S3. Log-rank p-values in the training (left column) and test cohorts (right column) of CPHMs built using

(a) PH-CT, (b) PH-PET, and (c) PH-PET/CT signatures.

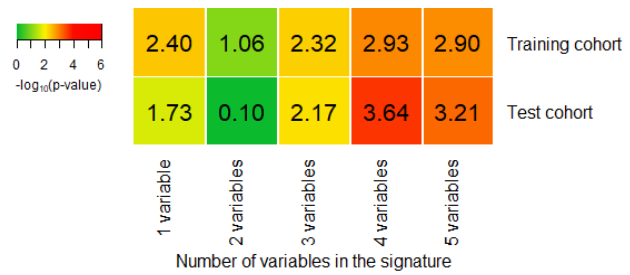


Figure S4. Log-rank p-values in the training and test cohorts of CPHMs built using clinical signatures.

REFERENCES

1. Haralick, R.M.; Shanmugam, K.; Dinstein, I. Textural features for image classification. *IEEE Trans. Syst. Man Cybern.* **1973** 3:610-621. [10.1109/TSMC.1973.4309314](https://doi.org/10.1109/TSMC.1973.4309314)
2. Assefa, D.; Keller, H.; Ménard, C.; et al. Robust texture features for response monitoring of glioblastoma multiforme on T1-weighted and T2-FLAIR MR images: A preliminary investigation in terms of identification and segmentation. *Med. Phys.* **2010** 34(4): 1722-36. <https://doi.org/10.1118/1.3357289>
3. Thibault, G. Indices de formes et de textures: de la 2D vers la 3D. Application au classement de noyaux de cellules *PhD Thesis* University AIX-Marseille, France, 2009.
4. Aerts, H.J.W.L.; Velazquez, E.R.; Leijenaar, R.T.H.; et al. Decoding tumour phenotype by noninvasive imaging using a quantitative radiomics approach. *Nat. Commun.* **2014** 2014; 5: 4006. <https://doi.org/10.1038/ncomms5006>
5. Galloway, M.M. Texture analysis using gray level run lengths. *Comput. Graph. Image Process.* **1975** 4:172-179. [https://doi.org/10.1016/s0146-664x\(75\)80008-6](https://doi.org/10.1016/s0146-664x(75)80008-6)
6. Chu, A.; Sehgal, C.; Greenleaf, J. Use of gray level distribution of run lengths for texture analysis. *Pattern Recognit. Lett.* **1990** 11:415-419. [https://doi.org/10.1016/0167-8655\(90\)90112-f](https://doi.org/10.1016/0167-8655(90)90112-f)
7. Dasarathy, B.; Holder, E. Image characterizations based on joint gray-level run length distributions. *Pattern Recognit. Lett.* **1991** 12:497-502. [https://doi.org/10.1016/0167-8655\(91\)80014-2](https://doi.org/10.1016/0167-8655(91)80014-2)
8. Thibault, G.; Fertil, B.; Navarro, C.; et al. Texture indexes and gray level size zone matrix: application to cell nuclei classification Pattern Recognition and Information Processing (PRIP), Minsk, Belarus, 2009.
9. Amadasun, M.; King, R. Textural features corresponding to textural properties. *IEEE Trans. Syst. Man Cybern.* **1989** 19:1264–1274. <https://doi.org/10.1109/21.44046>
10. Sun, C.; Wee, W.G. Neighboring gray level dependence matrix for texture classification. *Comput. Vision Graph Image Process* **1983** 23:341-352. [https://doi.org/10.1016/0146-664x\(82\)90093-4](https://doi.org/10.1016/0146-664x(82)90093-4)